1978

A Mathematical Model Of Placental Blood Flow.

Howard William Perlis
University of Alabama at Birmingham

A MATHEMATICAL MODEL OF PLACENTAL BLOOD FLOW

by

HOWARD WILLIAM PERLIS

A DISSERTATION

Submitted in partial fulfillment of the requirements
for the degree of Doctor of Philosophy in the
Division of Biophysical Sciences in the Graduate School,
University of Alabama in Birmingham

BIRMINGHAM, ALABAMA
1978

ACKNOWLEDGEMENTS

It is a privilege and a pleasure to acknowledge the support and guidance given to me by Dr. Josiah Macy, Jr. It is impossible to detail the many ways his ideas have influenced mine over the past twelve years, but my debt is profound.

Gratitude is also due to Dr. Charles E. Flowers, Jr. for his support and encouragement of our fetal monitoring research. His conviction that interdisciplinary studies would benefit his patients led directly to this work.

TABLE OF CONTENTS

LIST OF FIGURES

LIST OF TABLES

INTRODUCTION

This dissertation will be concerned with the effects of uterine contractions on blood flow to and from the maternal side of the placenta. A fuller understanding of the interactions between the intrauterine forces required to deliver the fetus and the blood supply to the placenta would be of value to the obstetrician responsible for the delivery, and to the scientist interested in labor physiology.

The prime objective of the obstetrician is to deliver the healthiest possible babies to the healthiest possible mothers. The attainment of this objective requires continuous redefinition of what is meant by "healthy" as new knowledge of fetal and maternal physiology and pathology is acquired. New techniques of diagnosis and intervention are being developed almost daily and result in continual change (and hopefully, improvement) in the state of the art.

Labor and delivery are two of the most critical events of the entire pregnancy. Much effort has been expended towards making labor and delivery safer for both mother and fetus; recently the major emphasis has been to determine and modify the effects of the labor process on the oxygen supply to the fetus. Although the fetal oxygenation process is beyond the scope of this dissertation, it is reasonable to suppose a relationship between blood flow to the placenta and fetal oxygenation exists.

Disruption of the oxygen supply can have immediate grave consequences, such as fetal death or meconium aspiration. Longer term effects of decreased fetal oxygenation can be brain damage manifested, for example, as Cerebral Palsy, learning disorders or sensory deficits.

On the positive side, the labor and delivery period is the time when: physician-patient interaction is high, detection of problems is possible with fetal monitors and scalp blood samples, and interventions to speed up, circumvent or slow down labor are feasible.

For all these reasons, and because it is easier (but still difficult) to obtain data during this period rather than earlier in the pregnancy, advances in our knowledge of labor-fetal oxygen interactions have a potentially high impact on improving health care.

Since the oxygen is carried to the fetus via blood, an understanding of the oxygen transfer to the fetus must depend on an understanding of maternal, placental and fetal hemodynamics.

Research into the dynamics of placental blood flow has been hampered by the technical difficulties encountered in making meaningful measurements in animals and by the unavailability of non-invasive, non-hazardous measurement methods suitable for use with human subjects. While the uterine and umbilical cord hemodynamics have been explored quantitatively, our knowledge of the circulation of blood in the maternal side of the placenta is qualitative.

As an aid to understanding the labor-blood flow interactions in the maternal side of the placenta, a mathematical model linking uterine contractions and maternal placental blood flow will be presented and discussed.

BACKGROUND

Blood Flow

In a series of experiments, Ramsey et al. (16) showed that, in the rhesus monkey, maternal blood from the uterus enters the intervillous space in geyser-like spurts from arterial inlets at the placental base. The blood then spreads laterally in the intervillous space where it bathes the capillary bed of the fetal side of the placenta. It is here that the major exchange of nutrients and wastes takes place between the fetus and its life support system. The maternal blood then drains into venous outlets, also located at the base of the intervillous space.

The effects of uterine contractions on the blood flow to the uterine myometrium and the maternal side of the placenta is still somewhat unclear.

Novy (13), using a radioactive microsphere technique, found that, in the rhesus monkey, a sustained contraction reduced blood flow to the placenta while increasing the blood flow to the uterine myometrium. Assali et al. (2), using calibrated electromagnetic flowmeters to measure total blood flow to the uterus of the pregnant ewe, found a marked decrease in flow in response to uterine contractions. Greiss (5), also using electromagnetic flowmeters, reported that total flow into the uterus was inversely proportional to the intrauterine pressure.

Flow out of the uterus and placenta was measured by Assali et al. (3) who found that increasing intrauterine pressure led to a drop in blood flow.

Although Novy (13) did not report quantitative measurements of blood flow, and the anatomical arrangement of the placenta precludes direct measurement of blood flow by the electromagnetic flowmeter, these experiments indicate that "normal" uterine contractions reduce the blood flow to and from the uterus and placenta.

Blood Volume

On the basis of cineangiographic evidence, Ramsey et al. (16) contended that the placental volume of the rhesus monkey did not decrease during a uterine contraction. In a direct attack on the problem of uterine blood volume, Abrams et al. (1) gave nonpregnant ewes progesterone and estrogen prior to surgery, inducing a large, well perfused and contractile uterus. The dissected but still perfused uterus was weighed during a series of contractions (spontaneous and oxytocin induced). A direct relationship between the force of the contraction and the weight of the uterus was found. Because the ewes were not pregnant, this experiment clearly shows that blood is sequestered in the uterine myometrium during a contraction. That the blood volume of the human placenta increases during a contraction was demonstrated by Scheffs et al. (17), utilizing radioactive iodinated human serum albumin in order to locate the placenta during labor. These measurements showed that placental blood volume increased about 23% over the baseline volume during contractions of 55 mmHg intensity.

In summary, the available information indicates that during a "normal" uterine contraction blood flow to and from the uterine myometrium and the placenta decreases, while the blood volume of the myometrium and placenta increases.

Uterine Shape

The shape of the full term uterus has been described as ovoid (6). During a contraction, it is the upper part of the uterus which actually contracts, forcing the fetus downward towards the outside world. The lower part of the uterus relaxes to accommodate the fetal presenting part (usually the head) (7).

Mathematical Models

In an attempt to model the maternal placental blood volume increase during contractions, which they had observed in their experiments, Scheffs et al. (17) assumed that blood flow into and out of the placenta obeyed the Poiseuille-Hagen formulation for flow in rigid tubes where flow is proportional to pressure divided by resistance. The blood flow was controlled by inlet and outlet valves which were either fully open or fully shut depending on the pressure exerted by the contraction. Proper choice of the parameters enabled the model to simulate the increase in placental blood volume which had been observed. Fig. 1 illustrates the valve design of the model.

The major significance of this model is the incorporation of the pressure multiplier constant K_3 in the valve operation equations (EQ. 1 and 2). Since the placenta is contained within the uterus, the placental pressure is the sum of the intrauterine pressure

Fig. 1 Simplified diagram of the relationship between the arterial pressure $P_1(t)$, the placental pressure $P_2(t)$ and the intra-uterine pressure $P_4(t)$.

Fig. 1

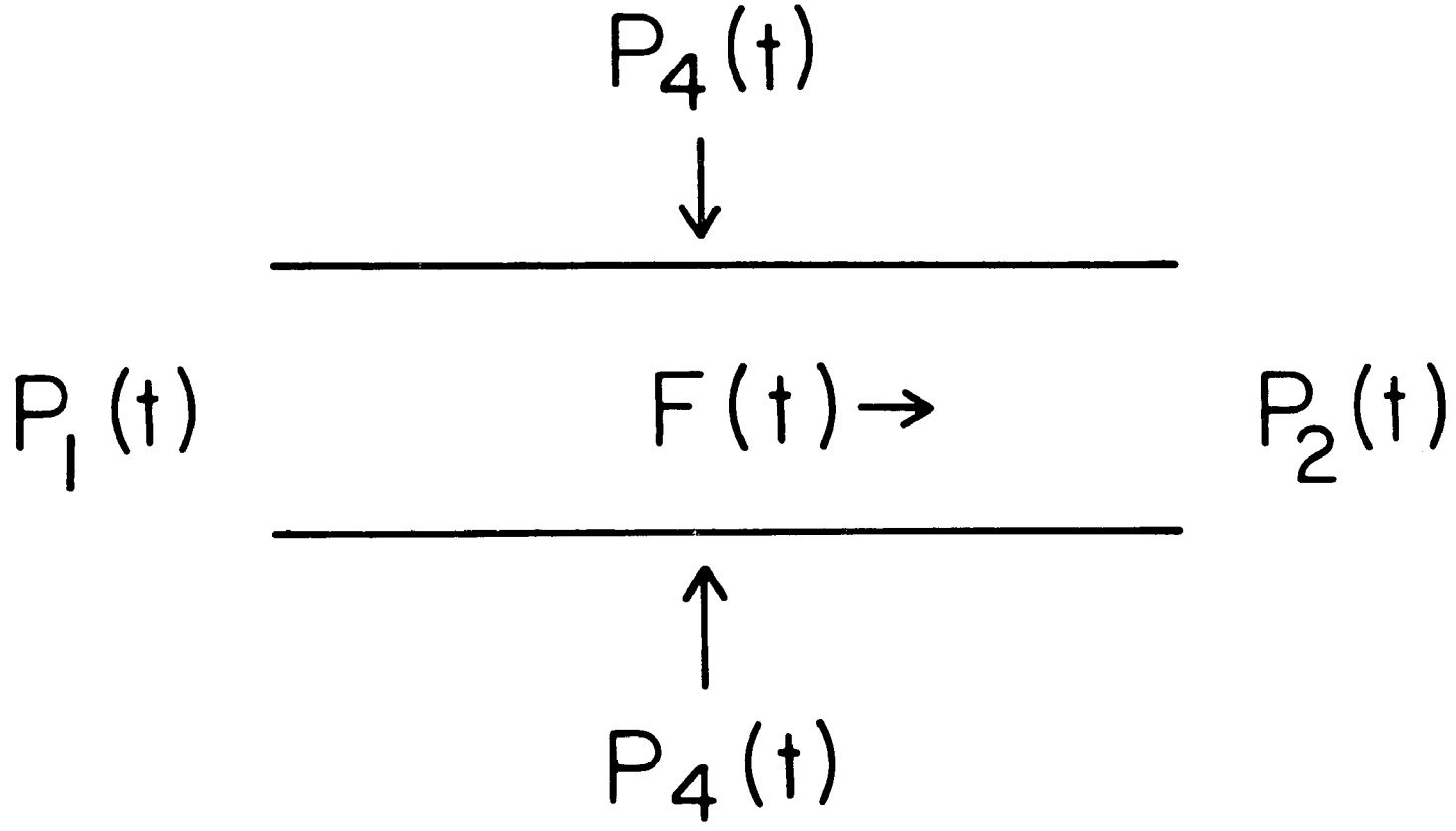

plus other factors. A model which assumes that the pressure which operates the valve mechanism is the same as the intrauterine pressure will show a decrease in placental volume during a contraction as the flood is squeezed out of the placenta.

$$F(t) \propto P_1(t) \quad \text{when} \quad P_1(t) > K_3 P_4(t) \qquad \text{EQ. 1}$$

$$F(t) = \text{Zero} \quad \text{when} \quad P_1(t) < K_3 P_4(t) \qquad \text{EQ. 2}$$

The limitations of this model are: the lack of justification for the incorporation of binary state (open or shut) valves in order to control the blood flow and the assumption of constant placental compliance.

Values of the pressure multiplier and other variables affecting the behavior of the model and the function used to generate the uterine contraction waveform were not reported.

It has been suggested by Power (15) that "sluice" flow might be an appropriate formulation for representing some of the factors affecting maternal placental blood flow.

"Sluice" flow theory, applying to thinwalled collapsible tubes subjected to surrounding pressures, has been utilized in research on pulmonary circulation (10), forearm circulation, thoracic blood flow (8) and the fetal placental circulation (15).

If the concepts of sluice flow are applied to the situation depicted in Fig. 1, the equations governing flow are EQ. 3, EQ. 4 and EQ. 5.

$$F(t) \propto P_1(t) - P_2(t) \quad \text{when} \quad P_1(t) > P_2(t) > P_4(t) \qquad \text{EQ. 3}$$

$$F(t) \propto P_1(t) - P_4(t) \quad \text{when} \quad P_1(t) > P_4(t) > P_2(t) \qquad \text{EQ. 4}$$

$$F(t) = \text{Zero} \quad \text{when} \quad P_4(t) > P_1(t) > P_2(t) \qquad \text{EQ. 5}$$

where $F(t)$ = blood flow

$P_1(t)$ = arterial pressure

$P_2(t)$ = placental pressure

$P_4(t)$ = intrauterine pressure

K_3 = pressure multiplier constant

In a recent mathematical model of placental blood flow and oxygen transport, Butler et al. (4) assumed that sluice flow concepts governed the outflow of blood from the maternal side of the placenta and that Poiseuille-Hagen theory described the inflow of blood. In this formulation the surrounding pressure was set equal to the intrauterine pressure. Placental volume curves obtained during simulation runs with this model were the reverse of those observed experimentally since the volume was reduced rather than increased during a contraction episode.

While the discrepancy between the model's behavior and experimentally obtained placental volume curves were not discussed in the paper, this result is a consequence of equating the pressure which operated the sluice mechanism and the intrauterine pressure, as has been previously discussed. Also not discussed was the reason for

using one formulation for the blood flow into the maternal placenta and a different formulation for the blood flow out of the maternal placenta.

MODEL DEVELOPMENT

A model was designed to simulate the essential features of the maternal placental circulation and the contractions of labor.

The model was constructed in four sections, an inlet section, a placental section, an outlet section and a contraction driving section. (See Fig. 2).

The inlet section is composed of the arterial pressure, the arterial resistance and the surrounding pressure generated by the uterine contraction.

The placental section incorporates the placental pressure, intrauterine pressure, placental compliance and placental volume.

The outlet section contains the venous resistance, venous pressure and the surrounding pressure.

The contraction driving section is composed of an arbitrary function designed to simulate, in simplified form, the pressures generated during a uterine contraction.

Model Assumptions

As in any attempt to construct a model, assumptions were made concerning many aspects of the real world situation being simulated.

Fig. 2 Sluice flow diagram illustrating the relationships defined by EQ. 6 through EQ. 18. The variables are defined in Table 1.

Fig. 2

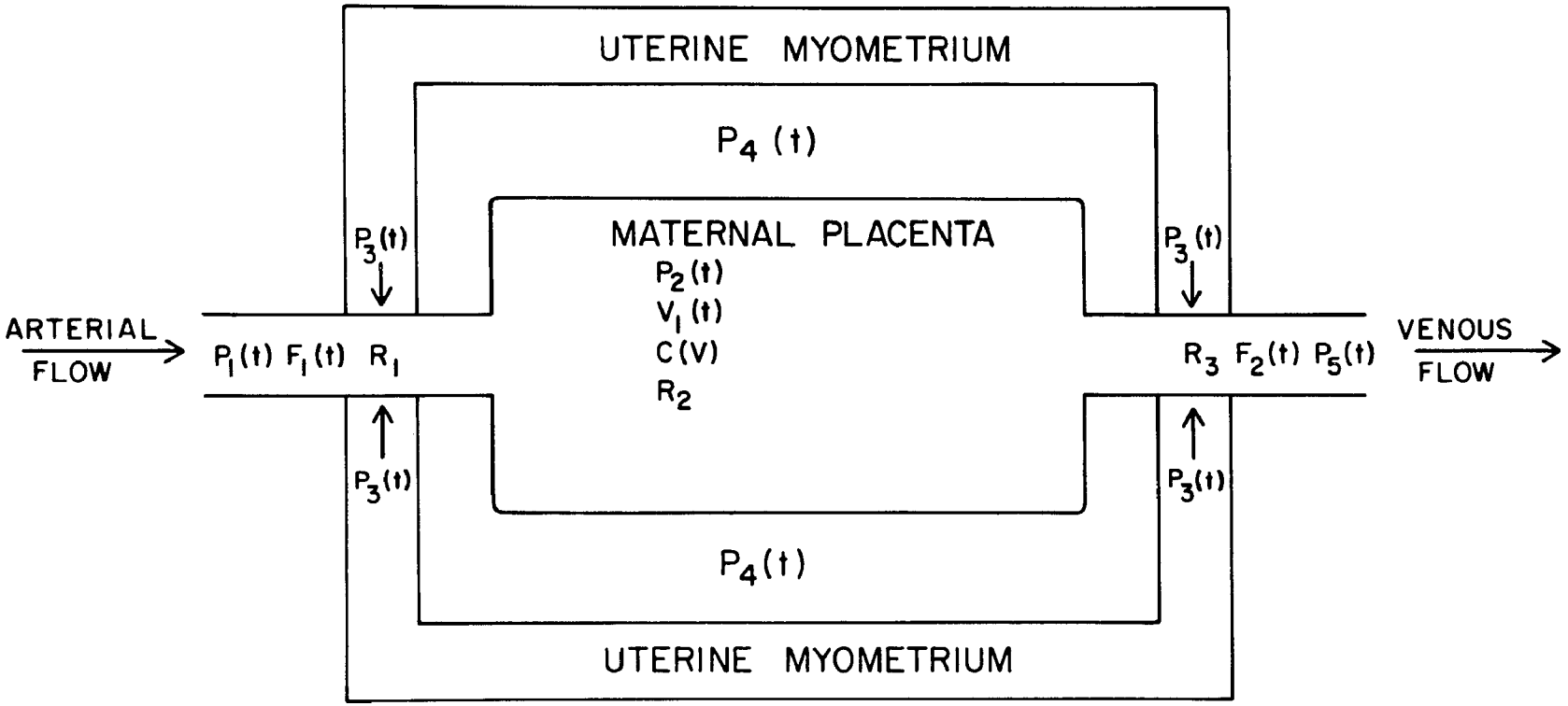
UTERINE MYOMETRIUM
P_4 (t)
P_3(t)
MATERNAL PLACENTA
P_2(t)
V_1(t)
C(V)
R_2
P_3 (t)
ARTERIAL FLOW
P_1(t) F_1(t) R_1
R_3 F_2(t) P_5(t)
VENOUS FLOW
P_3(t)
P_3(t)
P_4(t)
UTERINE MYOMETRIUM

The sluice mechanism previously discussed was assumed to be operative because of the anatomical relationship between the rather fine structure of the placenta and the heavy muscle wall of the uterus.

In the derivation of the relationship between the intrauterine pressure developed by the contraction and the surrounding pressure which drives the sluice flow mechanism, it was assumed that the region of the uterus at the location of the placenta can be represented by a portion of a sphere, in order to simplify derivation. (See Fig. 3)

The inlet and outlet ports were assumed to be circular because the cineangiographic experiments of Ramsey et al. (16) showed circular "smoke rings" during injection.

The pulsatile nature of blood flow to the uterus was not considered to be an important factor affecting the contraction-volume change relationship.

The placental compliance function chosen is an adaptation of a model of cardiac ventricular compliance developed by Turner (Malcolm E. Turner, Ph.D., Personal Communication). The function is flexible, features a relatively linear portion in the middle range of values and a rapid decrease in compliance at maximum volumes. (See Fig. 4)

Because there is, as yet, no agreement as to what characteristics comprise a typical uterine contraction or a typical labor pattern, an arbitrary, simplified pressure waveform function was created. (See Fig. 5)

This trapezoidal waveform generator allows easy, independent control over the baseline pressure (tonus), the duration of the

Fig. 3 Contraction diagram illustrating the relationship between the change in the radius of a portion of the uterus and the change in the radius of an inlet or outlet port of the placenta.

Fig. 3

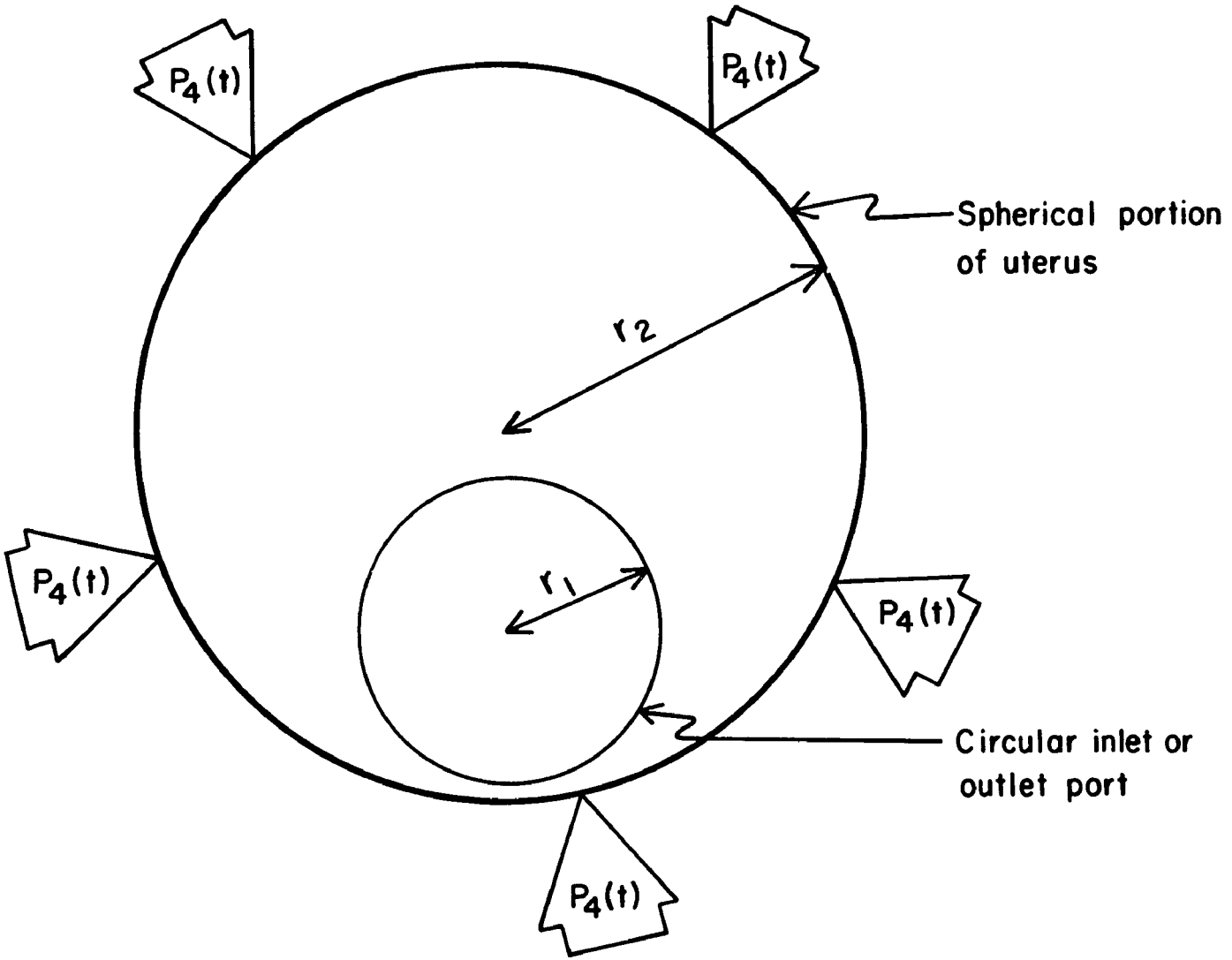
$P_4(t)$
$P_4(t)$
Spherical portion of uterus
r_2
$P_4(t)$
r_1
$P_4(t)$
Circular inlet or outlet port
$P_4(t)$

Fig. 4 Placental compliance $C(V_1)$ versus placental volume $V_1(t)$ for various values of δ, with $\delta = 3$ and $V_2 = 100$ ml.

Fig. 4

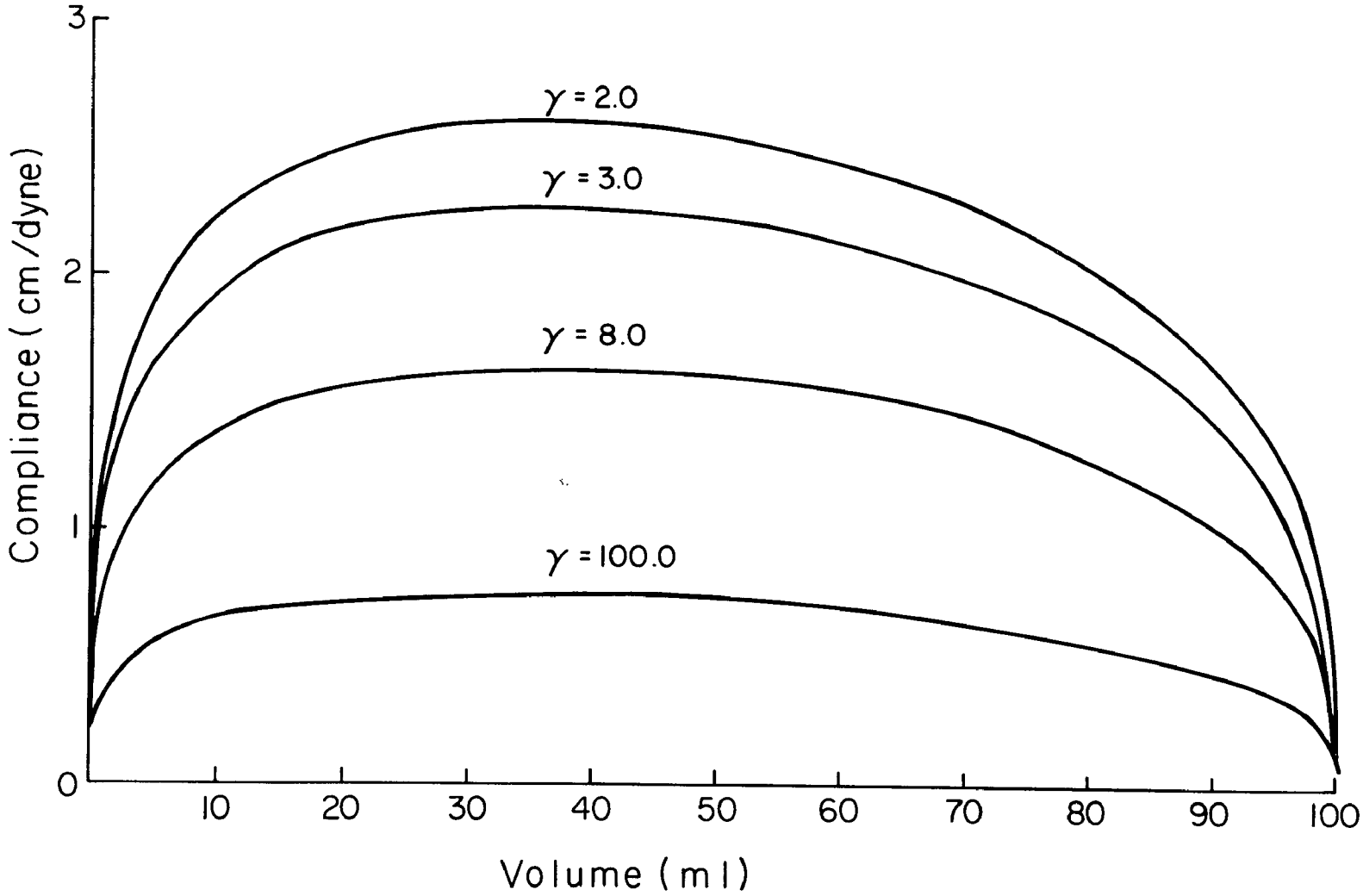
3
2
1
0
Compliance (cm /dyne)
γ = 2.0
γ = 3.0
γ = 8.0
γ = 100.0
10
20
30
40
50
60
70
80
90
100
Volume (ml)

Fig. 5 Intrauterine pressure $P_4(t)$ developed during a typical contraction.

Fig. 5

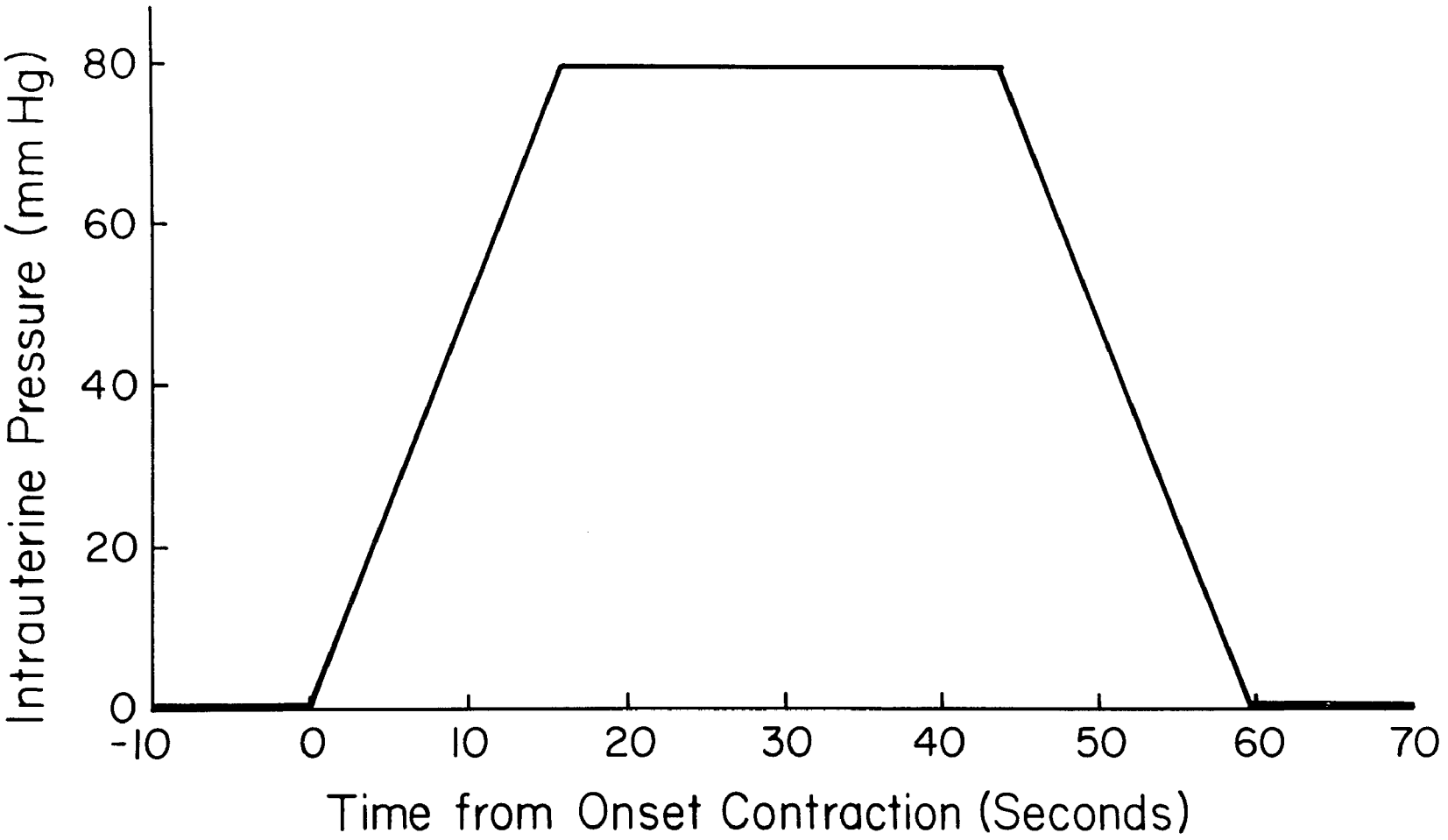
Intrauterine Pressure (mm Hg)
80
60
40
20
0
-10
0
10
20
30
40
50
60
70
Time from Onset Contraction (Seconds)

contraction, the peak pressure reached, the rate of pressure increase and decrease and the frequency of repetition. The method of generation (EQ. 17) is analogous to the method used to generate triangle waves in an electronic function generator.

Exclusions

Excluded from consideration or incorporation in this model of placental blood flow were the effects of uterine contractions on the fetal side of the placenta, the umbilical cord and the fetus itself.

MODEL CONSTRUCTION

The set of equations governing the operation of the model and the definitions of the variables follows. (See Table 1 for definitions)

Inlet Section Equations

The inlet section equations were formulated according to sluice flow principles. When the uterine tonus is low, and the conditions of EQ. 6 are met, the blood flow is governed by classical Poiseuille-Hagen theory.

$$F_1(t) = (P_1(t) - P_2(t)) \;/\; (R_1 + R_2) \quad \text{when } P_1(t) > P_2(t) > P_3(t) \text{ or } P_2(t) > P_1(t) > P_3(t) \qquad \text{EQ. 6}$$

It should be noted that $P_3(t)$ plays no part in the regulation of the blood flow at this stage.

As the contraction increases in intensity, $P_3(t)$ increases until the conditions of EQ. 7 are satisfied.

$$F_1(t) = (P_1(t) - P_3(t)) \;/\; (R_1 + R_2) \text{ when } P_1(t) > P_3(t) > P_2(t) \qquad \text{EQ. 7}$$

At this point in the contraction the sluice mechanism becomes operative and $P_2(t)$ does not affect the blood flow.

TABLE 1

Definitions of Model and Program Symbols

SYMBOL	CSMP NAME	DEFINITION	VALUE	DIMENSIONS*	UNITS
$P_1(t)$	ARTP	Arterial Pressure	100	$M \cdot L^{-1} \cdot T^{-2}$	mmHg
$P_2(t)$	PLACP	Placental Pressure	See Fig. 9	$M \cdot L^{-1} \cdot T^{-2}$	mmHg
$P_3(t)$	SQ1	Effective Sluice Pressure	See Fig. 6	$M \cdot L^{-1} \cdot T^{-2}$	mmHg
$P_4(t)$	SQUEEZ	Intrauterine Pressure	0-80	$M \cdot L^{-1} \cdot T^{-2}$	mmHg
$P_5(t)$	VENP	Venous Pressure	10	$M \cdot L^{-1} \cdot T^{-2}$	mmHg
R_1	ARTR	Arterial Resistance	40000	$M \cdot L^{-4} \cdot T^{-1}$	fluid ohms
R_2	PLACR	Placental Resistance	40000	$M \cdot L^{-4} \cdot T^{-1}$	fluid ohms
R_3	VENR	Venous Resistance	40000	$M \cdot L^{-4} \cdot T^{-1}$	fluid ohms
$F_1(t)$	FLIN	Flow into Placenta	See Fig. 7	$L^3 \cdot T^{-1}$	ml/sec
$F_2(t)$	FLOUT	Flow out of Placenta	See Fig. 10	$L^3 \cdot T^{-1}$	ml/sec
$C(V_1)$	COMPLI	Placental Compliance	See Fig. 4	$M^{-1} \cdot L^4 \cdot T^2$	cm/dyne
$V_1(t)$	PLAVOL	Placental Volume	See Fig. 8	L^3	ml
V_2	VMAX	Max. Placental Volume	100	L^3	ml

TABLE 1 (continued)

Definitions of Model and Program Symbols

SYMBOL	CSMP NAME	DEFINITION	VALUE	DIMENSIONS*	UNITS
γ	Gamma	Constant	See Fig. 12	L^3	ml
δ	Delta	Constant	3	--	--
α	--	Constant	1	$M^{-1} \cdot L^4 \cdot T^2$	cm/dyne
K_3	KAY	Pressure Multiplier	See Fig. 11	$M^{-1/3} \cdot L^{-1/3} \cdot T^{-2/3}$	--
T_1	--	Contraction Start Time	0	T	seconds
T_2	--	Contraction Finish Time	60	T	seconds
P_L	PMAX	Maximum Pressure	80	$M \cdot L^{-1} \cdot T^{-2}$	mmHg
K_1	SLOPE	Slope Multiplier	300	$M \cdot L^{-1} \cdot T^{-3}$	mmHg/min
V_i	VOL	Initial Volume	90	L^3	ml

*M = Mass; L = Length; T = Time

When the contraction progresses to the point where $P_3(t)$ exceeds both $P_1(t)$ and $P_2(t)$, the blood flow ceases, as shown in EQ. 8.

$$F_1(t) = \text{Zero} \qquad \text{when } P_3(t) > P_1(t) > P_2(t) \quad \text{or} \quad P_3(t) > P_2(t) > P_1(t) \qquad \text{EQ. 8}$$

In the event the conditions of EQ. 9 occur, the sluice mechanism operates as shown in EQ. 9, with the blood flow reversing direction and $P_1(t)$ ceasing to have any effect on the flow.

$$F_1(t) = (P_3(t) - P_2(t)) \;/\; (R_1 + R_2) \text{ when } P_2(t) > P_3(t) > P_1(t) \qquad \text{EQ. 9}$$

Placental Section Equations

The compliance of the placenta is represented by EQ. 10, which is discussed later.

$$C(V_1) = \left(\frac{V_1(t)}{\gamma} \ln \left(\frac{V_2}{V_1(t)}\right)\right)^{1/\delta} \qquad \text{EQ. 10}$$

The placental pressure developed by the system is described by EQ. 11.

$$P_2(t) = \frac{V_{1(t)}}{C} + P_4(t) \qquad \text{EQ. 11}$$

The placental volume is obtained by integration of the net placental flow as shown in EQ. 12.

$$V_1(t) = \int_0^t (F_1(t) - F_2(t))\, dt + V_i \qquad \text{EQ. 12}$$

Outlet Section Equations

The outlet section equations are developed in exactly the same manner as the inlet equations previously presented. Each outlet equation is analogous to a corresponding inlet equation as follows:

$$F_2(t) = (P_2(t) - P_5(t)) \,/\, (R_2 + R_3) \quad \text{when } P_2(t) > P_5(t) > P_3(t) \text{ or } P_5(t) > P_2(t) > P_3(t) \qquad \text{EQ. 13}$$

EQ. 13 is identical in form to EQ. 6.

$$F_2(t) = (P_2(t) - P_3(t)) \,/\, (R_2 + R_3) \quad \text{when } P_2(t) > P_3(t) > P_5(t) \qquad \text{EQ. 14}$$

EQ. 14 corresponds to EQ. 7.

$$F_2(t) = \text{Zero} \quad \text{when } P_3(t) > P_2(t) > P_5(t) \text{ or } P_3(t) > P_5(t) > P_2(t) \qquad \text{EQ. 15}$$

EQ. 15 corresponds to EQ. 8.

$$F_2(t) = (P_3(t) - P_5(t)) \,/\, (R_2 + R_3) \quad \text{when } P_5(t) > P_3(t) > P_2(t) \qquad \text{EQ. 16}$$

EQ. 16 corresponds to EQ. 9.

Contraction Section Equations

The contraction waveform is generated by the integration of a square wave function followed by limiting the upper value of the resulting triangular waveform. It should be noted that the variables x and y in EQ. 17 play no part in the model beyond generating the initial square wave.

$$P_4(t) = K_1 \int_{T_1}^{T} (x + y)\, dt: \quad 0 < P_4(t) < P_L;$$

$$x = 0,\ y = 0 \text{ when } T < T_1,\ T > T_2$$

$$x = 1,\ y = 0 \text{ when } T_1 < T < T_1 + \left(\frac{T_2 - T_1}{2}\right)$$

$$x = 0,\ y = -1 \text{ when } \frac{T_1 + T_2}{2} < T < T_2 \qquad \text{EQ. 17}$$

The output of EQ. 17 is shown in Fig. 5.

The relationship between the sluice pressure and the intrauterine pressure is shown in EQ. 18. The derivation of this equation is detailed below.

$$P_3(t) = K_3(P_4(t))^{4/3} \qquad \text{EQ. 18}$$

Non-Isometric Contraction

The derivation of the relationship between the surrounding pressure $P_3(t)$ and the intrauterine pressure $P_4(t)$ is based on the concept of the non-isometric contraction. Since it is known that in a normal labor the fetus is expelled from the uterus at some point, and that each contraction forces the fetus downwards, if only

temporarily, it was assumed that each contraction caused a transient decrease in the radius of the spherical section at the placental location. If the region of the uterine wall where the placenta is implanted is considered to be spherical and the inlet and outlet ports of the placenta are assumed to be circular, then the relationship $P_3(t) = K_3(P_4(t))^{4/3}$ can be derived as follows. (See Fig. 3)

Let r_1 ≡ radius of uterus

r_2 ≡ radius of port

c ≡ circumference of uterus

v(t) ≡ volume of uterus

$$v(t) = 4/3\ \pi\ r_1^3,\ c = 2\ \pi\ r_1 \qquad \text{EQ. 19}$$

$$r_2 = k_1 c = 2\pi\ k_1 r_1 \quad \text{where} \quad k_1 \equiv \text{dimensionless constant} \qquad \text{EQ. 20}$$

$$r_1 = \left(\frac{3}{4\pi}\ v(t)\right)^{1/3} \qquad \text{EQ. 21}$$

$$r_2 = 2\pi\ k_1 \left(\frac{3}{4\pi}\right)^{1/3}\ v(t)^{1/3} \qquad \text{EQ. 22}$$

$$\text{then} \quad F(t) = \left(\frac{\pi \Delta P}{8\eta L}\right)\ \left(2\pi k_1\ \left(\frac{3}{4\pi}\right)^{1/3}\ (v(t)^{1/3})\right)^4 \qquad \text{EQ. 23}$$

(Poiseuille-Hagen Flow)

where: $F(t) \equiv$ flow

$\eta \equiv$ viscosity

$\Delta P \equiv$ pressure differential

$L \equiv$ length of port

$$v(t) \propto k_2/P_4(t) \qquad \text{EQ. 24}$$

$$\text{therefore: } F(t) = \left(\frac{\pi \Delta P}{8\eta L}\right) \left(2\pi k_1 \left(\frac{3}{4\pi}\right)^{1/3} \left(\frac{k_2}{P_4(t)}\right)^{1/3}\right)^4 \qquad \text{EQ. 25}$$

where $P_4(t) \equiv$ intrauterine pressure

$k_2 \equiv$ constant

$$\text{or } F(t) \propto (P_4(t))^{-4/3} \qquad \text{EQ. 26}$$

The application of this formulation to sluice flow can be accomplished by:

$$P_3(t) = K_3(P_4(t))^{4/3} \quad \text{where } K_3 \equiv \text{pressure multiplier} \qquad \text{EQ. 27}$$

Placental Compliance

Let x = mean radial displacement of edge from geometric center of placenta

$V_1(t) \equiv$ volume of placenta

$V_2 \equiv$ maximum volume of placenta

$k(V_1) \equiv$ stiffness function (dimensionless)

$C(V_1) \equiv$ compliance

$\gamma \equiv$ constant

$\delta \equiv$ constant

$\alpha \equiv$ constant

Assume:

$$V_1(t) \propto x^{\delta}, \delta = 3.0 \qquad \text{for sphere}$$

$$\gamma\delta V_1(t)k' - V_1(t)k^{\delta+1} + \gamma k^{-\delta} = 0 \quad \text{stiffness equation} \qquad \text{EQ. 28}$$

Solve for k and C, with terminal conditions

$$V_1(t) = V_2,\ 1/k = C = 0$$

$$k(V_1) = \left(\left(\frac{V_1(t)}{\gamma}\right) \ln\left(\frac{V_2}{V_1(t)}\right)\right)^{-1/\delta} \qquad \text{EQ. 29}$$

$$C(V_1) = \frac{\alpha}{k(V_1)} \qquad \text{EQ. 30}$$

A family of compliance curves produced by this function is shown in Fig. 4.

MODEL PERFORMANCE

The equations comprising the model were translated into the Continuous System Modelling Program (CSMP) language and the program was executed on an IBM 370 computer. Values for the CSMP program parameters were chosen on the basis of physiological reasonableness although the choices were arbitrary. (See Table 1)

Because there is no typical contraction waveform, the contraction generator parameters were chosen to create a pattern similar to that observed clinically during a strong, regular labor.

The same intrauterine pressure waveform was used for all computer runs. As can be seen in Fig. 5, the maximum allowable pressure was limited to 80 mmHg, with the time the pressure was elevated above zero mmHg set at 60 seconds. The pressure reached its maximum value 15 seconds from the start of the contraction and started to fall 30 seconds later.

The effective sluice pressure waveform shown in Fig. 6 followed the same time course as the intrauterine pressure, although the maximum pressure was higher and the rise and fall were non-linear due to the form of the coupling equation (EQ. 18).

Blood flow into the placenta, as seen in Fig. 7, showed an initial fall at the start of the contraction followed by an abrupt rise starting at 8 seconds from the contraction onset. At 17 seconds

Fig. 6 Effective sluice pressure $P_3(t)$ developed during a typical contraction ($K_3 = 0.8$).

Fig. 6


Effective Sluice Pressure (mm Hg)
300
250
200
150
100
50
0
-10
0
10
20
30
40
50
60
70
Time from Onset of Contraction (Seconds)

Fig. 7 Blood flow into the maternal side of the placenta $F_1(t)$ during a typical contraction.

Fig. 7

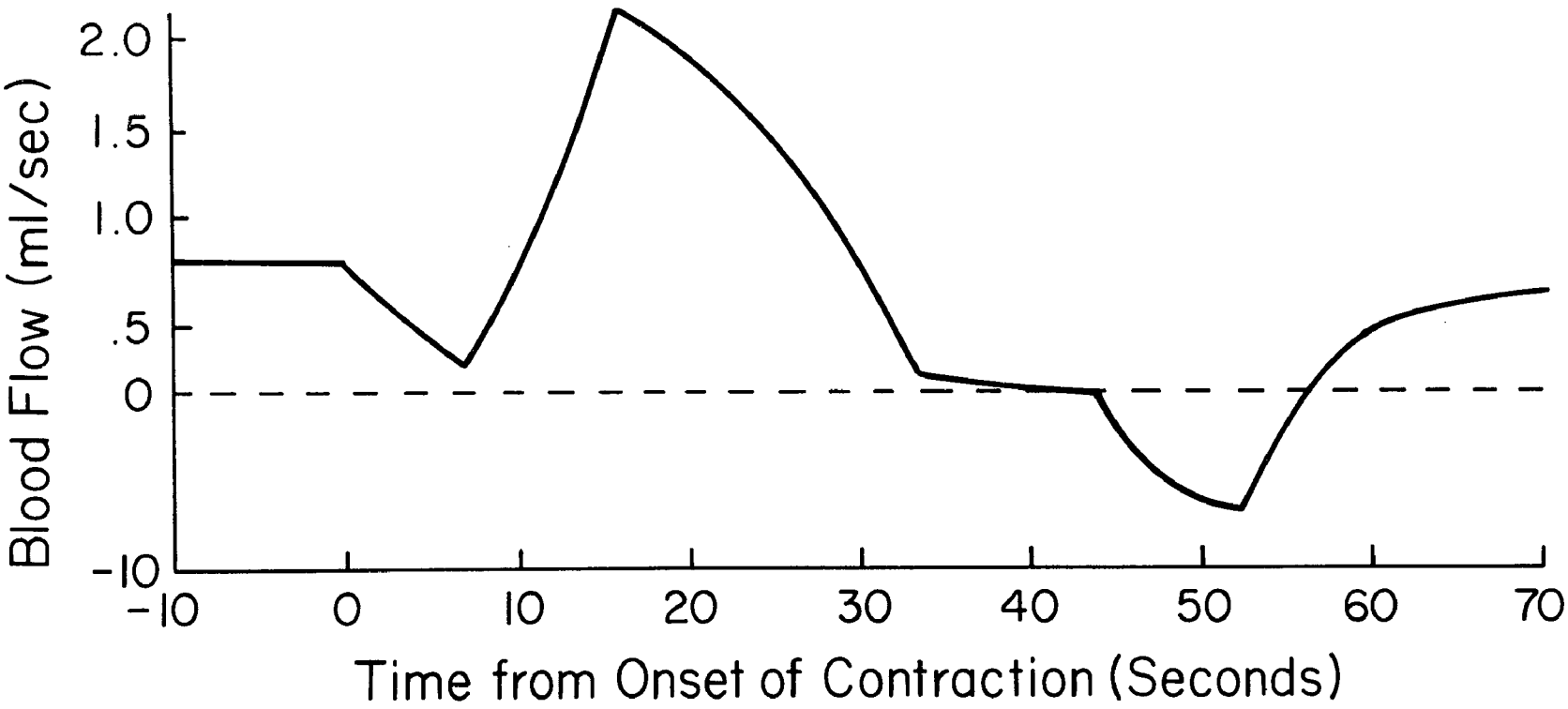
Blood Flow (ml/sec)
2.0
1.5
1.0
.5
0
-10
-10
0
10
20
30
40
50
60
70
Time from Onset of Contraction (Seconds)

from the contraction onset the flow starts to decrease, until it nears zero about 34 seconds from the contraction onset. At 45 seconds from the contraction onset the blood flow reverses for 12 seconds and then returns to its precontraction value.

The placental volume, shown in Fig. 8, increased gradually starting at 8 seconds from the contraction onset, reached a peak 38 seconds from the contraction onset and slowly returned to the precontraction value (not shown in Fig. 8) about 120 seconds later.

The placental pressure curve, shown in Fig. 9, rises until 45 seconds from the contraction onset. The pressure then falls sharply to precontraction values.

The blood flow out of the placenta, shown in Fig. 10, falls to zero shortly after the onset of the contraction and remains at zero until the contraction is almost finished. The outflow then overshoots the precontraction flow rate by 167%, later falling back to the precontraction level.

Fig. 8 Maternal placental blood volume $V_1(t)$ during a typical contraction.

Fig. 8

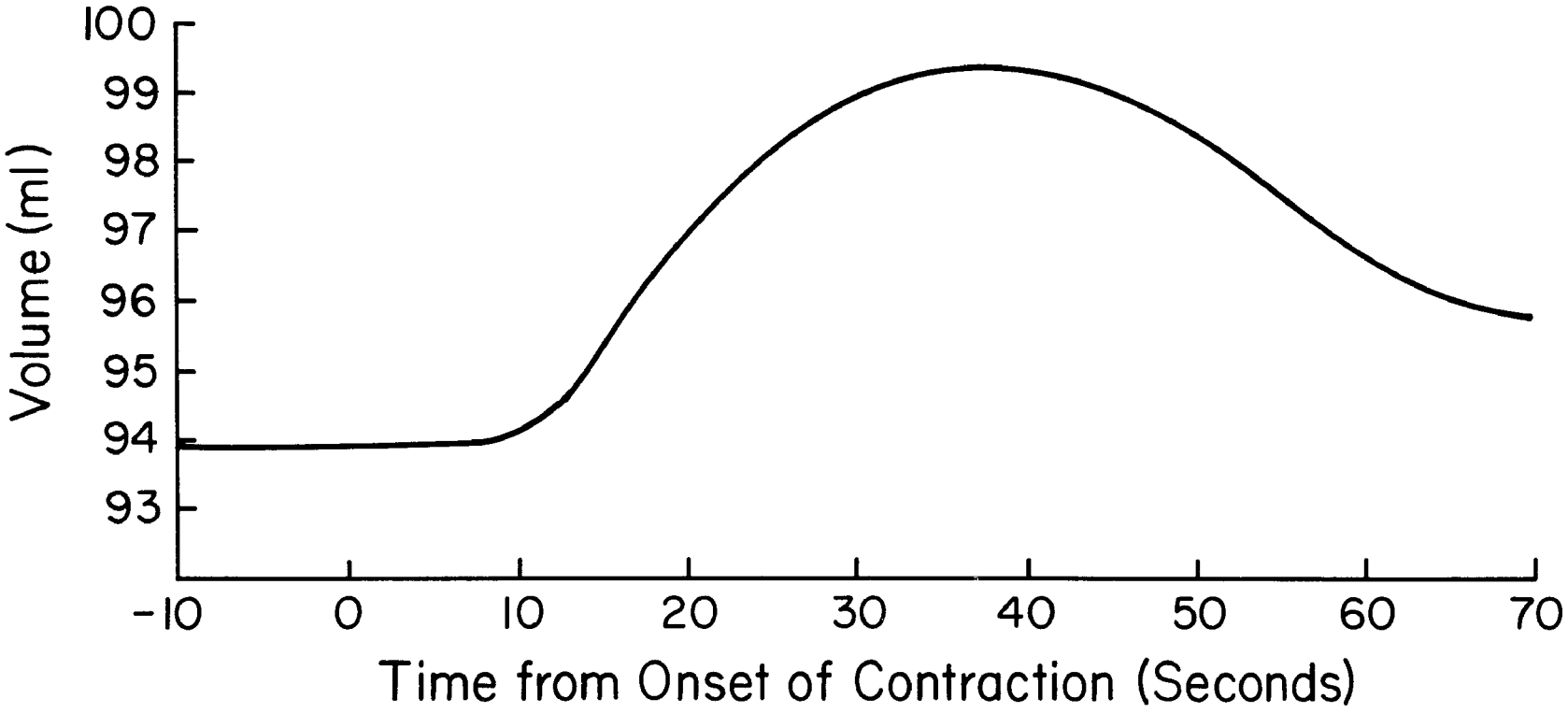
100
99
98
97
96
95
94
93
Volume (ml)
-10
0
10
20
30
40
50
60
70
Time from Onset of Contraction (Seconds)

Fig. 9 Maternal placental blood pressure $P_2(t)$ during a typical contraction.

Fig. 9


300
250
200
150
100
50
Pressure (mm Hg)
-10
0
10
20
30
40
50
60
70
Time from Onset Contraction (Seconds)

Fig. 10 Blood flow out of the maternal side of the placenta $F_2(t)$ during a typical contraction.

Fig. 10

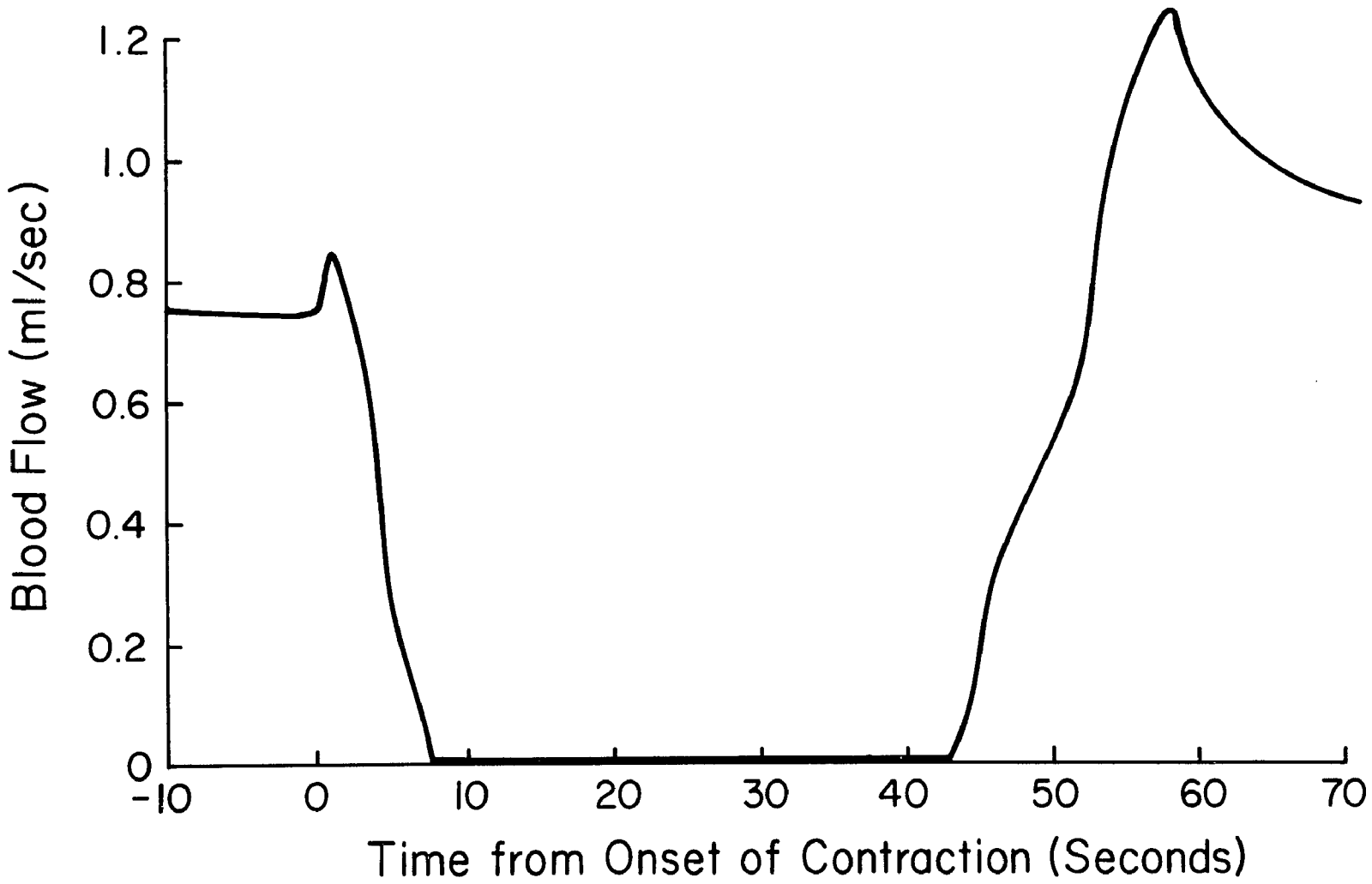
Blood Flow (ml/sec)
1.2
1.0
0.8
0.6
0.4
0.2
0
-10
0
10
20
30
40
50
60
70
Time from Onset of Contraction (Seconds)

DISCUSSION

Evaluation of Results

Integration Interval

The integration interval used for most of the simulations was 0.0063 second, which is the default value the CSMP program assigns for an output interval of 0.1 second. Trial runs were made with output intervals of 0.01 second and integration intervals of 0.00063 second without any increase in observable detail apparent in the graphs.

Simulation runs conducted with an output interval of 1.0 second and an integration interval of 0.063 second showed a considerable loss of information about the behavior of the intrauterine pressure waveform at its transition points. Since it was known that the intrauterine pressure curve changed slope abruptly, the output and integration intervals were decreased until the computer generated printer plots visually matched the required behavior of EQ. 17.

Sensitivity

The effect of the pressure multiplier K_3 on the relationship between the intrauterine pressure $P_4(t)$ and the effective sluice pressure $P_3(t)$ is shown in Fig. 11. Because of the exponential nature of EQ. 18, the effective sluice pressure increases rapidly

Fig. 11 Intrauterine pressure $P_4(t)$ versus the effective sluice pressure $P_3(t)$ for various values of the pressure multiplier K_3.

Fig. 11

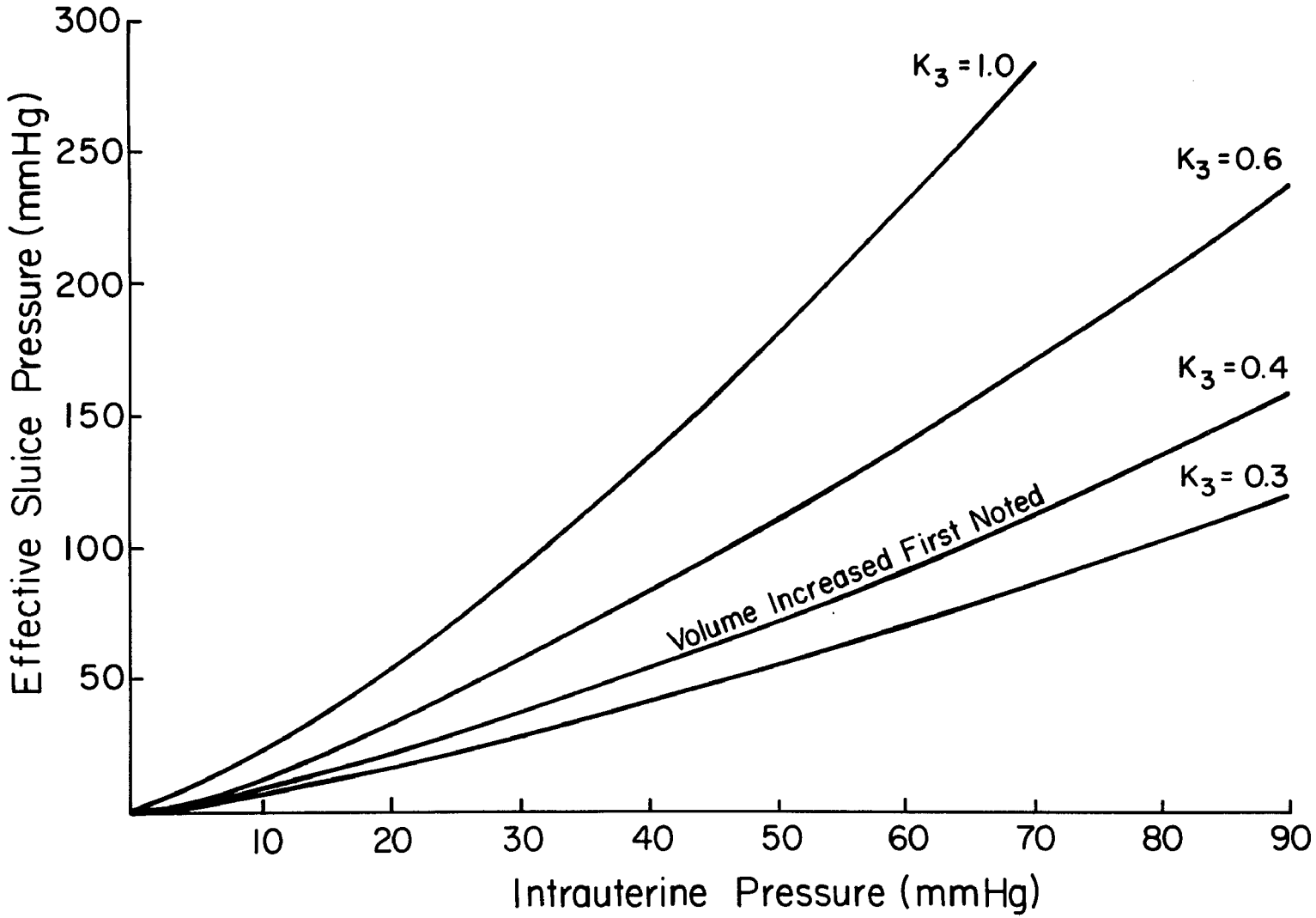
300
250
200
150
100
50
Effective Sluice Pressure (mmHg)
K_3 = 1.0
K_3 = 0.6
K_3 = 0.4
K_3 = 0.3
Volume Increased First Noted
10
20
30
40
50
60
70
80
90
Intrauterine Pressure (mmHg)

at higher intrauterine pressure values. The maternal placental volume increase was first noted when K_3 exceeded 0.4, when the effective sluice pressure did not exceed 200 mmHg at its peak.

The effect of varying the arterial pressure $P_1(t)$ on the placental volume is shown in Table 2.

TABLE 2

Arterial Pressure Versus Placental Volume

Arterial Pressure $P_1(t)$	Placental Volume $V_1(t)$	
	Precontraction Volume	Peak Volume
50	83.9	93.5
60	86.9	95.6
70	89.4	96.8
80	91.3	97.6
90	92.8	98.1
100	93.9	98.3

It can be seen that a 100% increase in the arterial pressure produced an 11.9% increase in the precontraction placental volume and a 5.1% increase in the peak volume. It can also be seen that as the arterial pressure is incremented upwards the rate of change in the precontraction and peak volume decreases.

The effect of varying the peak intrauterine pressure on the placental volume is shown in Table 3.

TABLE 3

Intrauterine Pressure Peak Versus Placental Volume Peak

Intrauterine Pressure $P_3(t)$ Peak	Placental Volume $V_1(t)$ Peak
10	93.6
20	94.7
30	95.2
40	96.1
50	97.4
60	98.3
70	98.8
80	99.2
90	99.4

It can be seen that large changes in the intrauterine pressure peak were not reflected in large changes in the placental volume peak and that the rate of change of the volume peak decreased with increasing pressure.

The sensitivity of the placental volume to changes in the pressure multiplier K_3 linking $P_3(t)$ and $P_4(t)$ is shown in Table 4.

TABLE 4

Pressure Multiplier versus Placental Volume Changes

Pressure Multiplier (K_3)	Maximum % Deviation from Precontraction Placental Volume
0.1	-12.5
0.2	- 9.2
0.3	- 5.8
0.4	- 1.4
0.5	2.3
0.6	4.4
0.7	5.5
0.8	5.9
0.9	6.0
1.0	6.1

The placental volume increase required for the model to agree with the experimentally determined volume increase occurred when the pressure multiplier exceeded 0.4. The higher values of K_3 had less of an effect on placental volume than did the lower values.

The variable with the greatest effect on placental volume is the compliance equation (EQ. 10) variable, γ. The change in placental volume during a contraction as γ varies is shown in Fig. 12.

It can be seen that the placental volume response to a contraction primarily depends on K_3 for direction and on γ for magnitude.

Fig. 12 Maximum maternal placental blood volume changes during a typical contraction versus the compliance variable δ.

Fig. 12

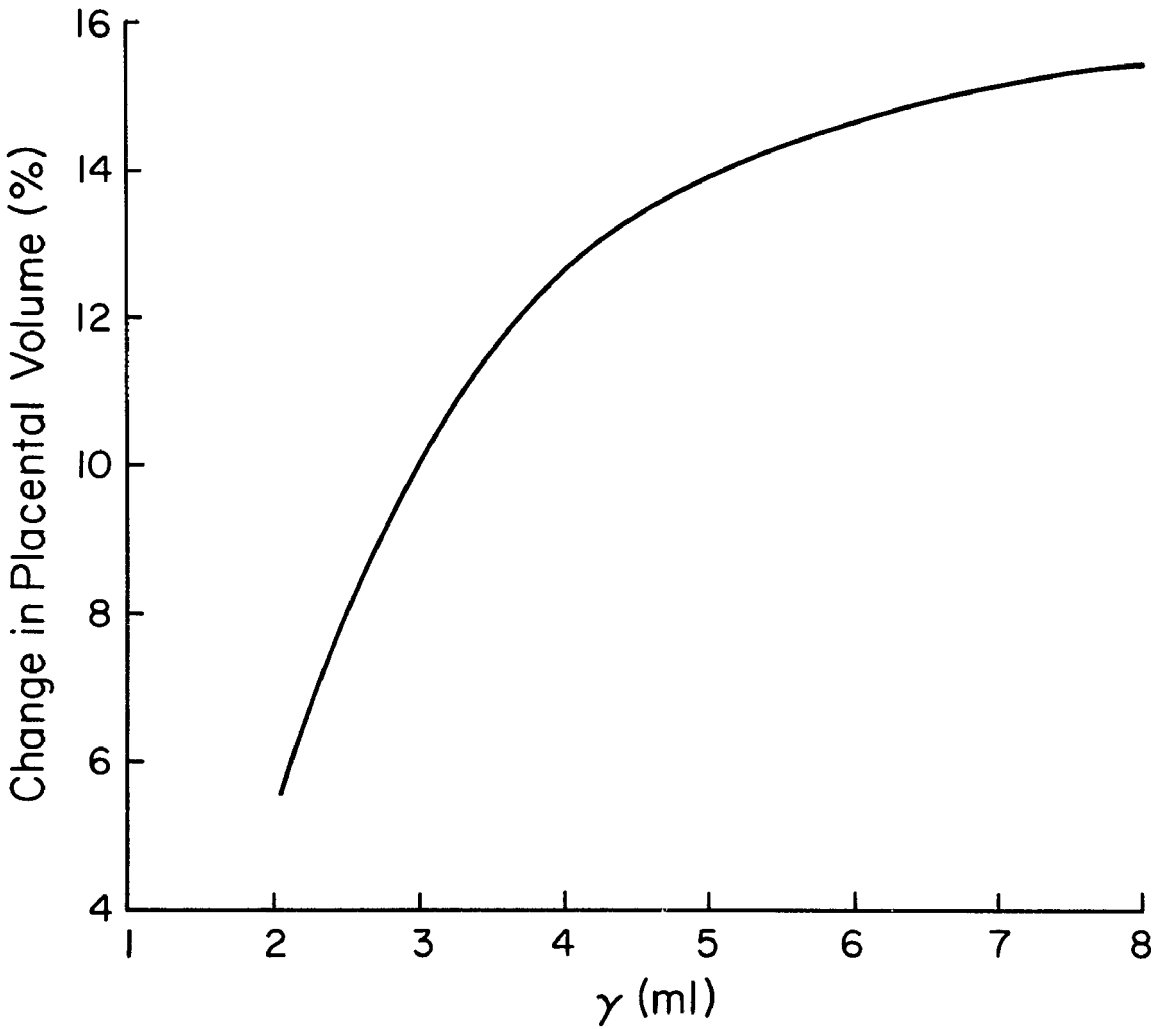

In all cases the model responded smoothly to changes in variable values with no oscillatory behavior found.

Comparison to Experimental Data

Comparison of the placental volume curve of Fig. 8 with that of Fig. 13 (from Scheffs et al. (17)) enables qualitative similarities between the model output and the experimental data to be seen.

Quantitative differences between the model output and the experimental data can be found in two areas. The first difference is in the maximum change in placental volume observed during a contraction. Scheffs et al. (17) reported that in normal, healthy patients the average change in placental volume equaled 23%. The greatest placental volume change the model produced was about 15%. This smaller volume change does, however, encompass the 12% volume change reported by Scheffs et al. (17) for preeclamptic patients. The difference in placental volume changes between the calculated values and the observed values might be eliminated by modification of the compliance equation (EQ. 10) parameters or the form of the equation itself, since the placental compliance is the major factor influencing the magnitude of the volume change.

The other major difference in model behavior versus observed behavior is in the time course of the placental volume changes. The calculated placental volume reached a peak 38 seconds from the onset of the contraction, while the observed placental volume reached its peak about 45 seconds from the start of the contraction (Fig. 13). Direct comparison of the time courses is made difficult because the contraction waveforms are 120 seconds long as reported by Scheffs et al.

Fig. 13 Maternal placental blood volume versus intrauterine pressure changes observed in humans. Adapted from Scheffs et al. (17).

Fig. 13

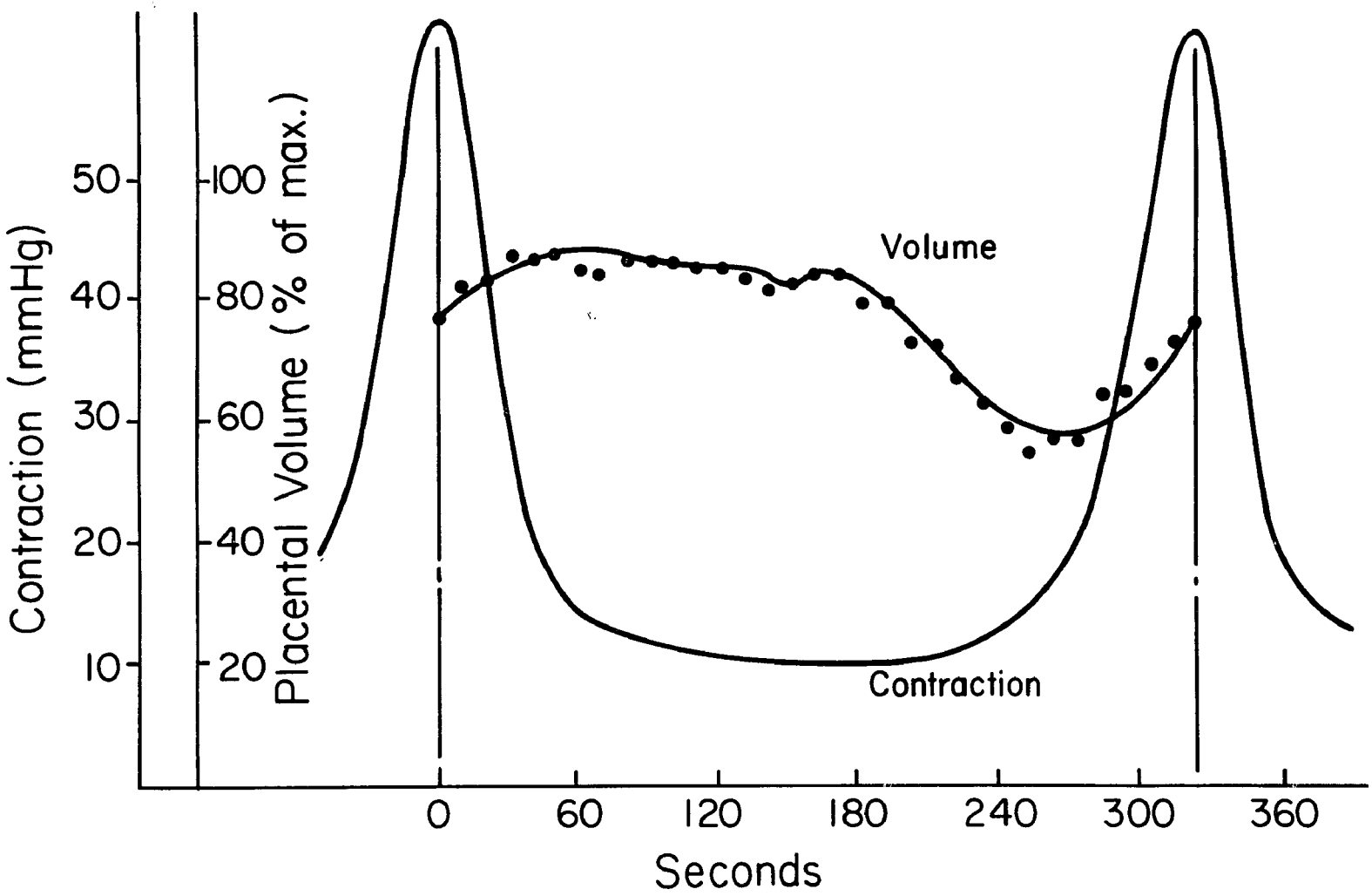
Contraction (mmHg)
50
40
30
20
10
100
80
60
40
20
Placental Volume (% of max.)
Volume
Contraction
0
60
120
180
240
300
360
Seconds

and 60 seconds in duration in this model. Variations in the arterial (R_1), placental (R_2) and venous (R_3) resistances in the model might reduce the time course differences. It should be noted that during the observation of several thousand contractions recorded on fetal monitors, the author has never seen a contraction longer than 100 seconds in duration.

An area of concern is the peak placental pressure generated during a contraction. In the example presented in Fig. 9 this pressure reaches a value 3.4 times the intrauterine pressure or about 275 mmHg. This pressure is the sum of the intrauterine pressure and the interaction between placental volume and compliance as shown in EQ. 11; thus the net placental pressure is about 195 mmHg. It might be the case that this rather high but still physiologically feasible pressure is a contributory factor in cases of placental abruption.

Unfortunately, there is little quantitative information available concerning actual blood flow rates into and out of the maternal side of the placenta to compare the calculated flow rates to. It can only be said that the complete cessation of blood flow seen in Figs. 7 and 10 near the midpoint of the contraction agrees with the blood flow data of Novy (13) gathered in experiments on the rhesus monkey.

Clinical Implications

The simulations demonstrate that the uterine volume changes that deliver the fetus may be responsible for some of the alterations in placental blood flow and volume observed during labor.

If the simple assumption is made that the oxygen available for transfer to the fetal circulation is proportional to the average maternal placental blood flow, it can be seen that towards the mid-point of a contraction, when flow in and out of the placenta ceases, the fetus is supplied with oxygen from a fixed volume of blood. (See Figs. 7, 8, 10.) If the oxygen consumption exceeds the supply, fetal compromise may occur, with possible grave consequences.

Although there are no continuous data available concerning fetal oxygenation, Myers (12) has described several quantitative relationships relating intrauterine pressure to fetal arterial pO_2, fetal heart rate and fetal brain damage in the rhesus monkey. It has also been shown that these relationships have some applicability to the human fetus (14, 9) undergoing the stress of labor, although much work remains to be done in this area. The model could be extended to encompass the transfer of maternal oxygen to the fetus and the removal of carbon dioxide from the fetus. If sufficient data could be gathered to allow reliable parameter estimation, the model could be used to identify an optimum labor pattern. An optimum labor pattern should provide enough interference with essential blood flows to help mature the fetal lungs, but not enough to depress the baby. It should deliver the baby fast enough to avoid exhausting the mother, but not so rapidly as to rupture the uterus or lacerate the cervix.

The results of this investigation imply that prolonged contractions interrupt blood flow to the maternal side of the placenta. For the clinician, this means that oxytocin administration must be carefully controlled. Furthermore, since the external contraction sensors supplied with fetal monitors give rather crude indications of

contraction strength and duration, the extra time and effort required to use the calibrated internal transducer could be repaid by a usable increase in information about the labor. For example, if the resting tonus exceeded the nominal 10 to 15 mmHg pressure estimated for the placental venous pressure, the clinician should be alerted to the possibility that blood flow is being compromised, and a closer watch should be kept on the patient and the fetal monitor.

Because the abdominal muscles can, when contracted, raise the measured intrauterine pressure, the simulation results imply that a reduction in anxiety (and therefore muscle tension) might have a direct effect on blood flow.

Experimentation to determine the effect of various relaxation techniques employed by the mother on intrauterine pressure, post-delivery Apgar scores and fetal blood gas composition is being planned.

The high placental pressures generated by the model might be implicated in cases of placental detachment and hemorrhage. In most labors this pressure might be tolerated without ill effect but in a smaller number of patients the pressures might exceed a physiologically safe limit. Animal research could quantify the placental pressures developed during the labor. Since the placental pressure is greatly influenced by the placental compliance, the interaction between the two will also have to be investigated.

Future Research

Spherical Assumption

Further investigation is needed to refine the relationship derived between the surrounding pressure controlling the sluice mechanism and the intrauterine pressure developed by the contraction.

It is obvious that the uterus is not a simple sphere. The coupling equation which has been derived (EQ. 18) is applicable to near-spherical shapes such as an ellipsoid through modifications to the pressure multiplier K_3. More complicated shapes and the incorporation of other factors such as the shifting of muscle layers or thickening of the uterine wall during a contraction can be accommodated by generalizing the coupling equation.

It would appear that some of the advanced techniques developed recently in the fields of ultrasonic imaging and computer tomographic scanning could be used to obtain a more detailed and realistic view of the uterus at rest and during a contraction. This information would allow the creation of a coupling equation which would be a more accurate representation of the forces involved in the control of blood flow.

Non-Pulsatile Blood Flow Assumption

This model assumed non-pulsatile blood flow. It has been pointed out by Blackstone that while the average volume change due to pulse effects may be negligible, the instantaneous effects can have a considerable influence on the oxygen transfer to the fetus, analogous to that noted in babies with certain cardiac defects (Eugene H. Blackstone, M.D. Personal Communication).

Future models should incorporate pulsatile blood flow in order to investigate oxygen transfer and the more subtle flow effects neglected in the current model.

Placental Volume and Compliance

Since the model proved to be most sensitive to changes in the values of the placental compliance function variables, a more extensive investigation of its behavior with different compliance functions is indicated. The compliance function used in this model assumed a spherical intervillous space ($\delta = 3$). It is quite possible that δ is a function of placental distension and should be investigated in the model. Since there seems to be no information available concerning actual placental compliance, experimentation in this area is needed.

It is unlikely that the use of techniques involving the administration of radioactive materials to pregnant women in order to gain information about placental volume would be allowable under current human use guidelines. Since placental localization can be accomplished quickly and safely by ultrasonic methods, Scheffs' experiment is not repeatable. More information is needed concerning placental volume, but this information will have to be gathered via ultrasonic imaging on the human.

The investigation of placental compliance in the human would also require the use of non-invasive techniques yet to be developed. It is possible that in-vitro experimentation with freshly delivered placentas might provide adequate information for the development of a realistic compliance function.

Contractions

While this model used a simplified contraction waveform, in actual labors no patient has the same contraction pattern as another, nor does any one patient have successive identical contractions. A set of intrauterine pressure curves representing a typical labor, agreed upon by a majority of researchers in the field, could be extremely useful. It might also be possible, by pooling data, to create a standardized set of atypical labor patterns.

The major contributions of a widely used standard set of uterine contraction waveforms would be to make the understanding of other researchers' work far easier, and to reduce the amount of computer usage now needed to compare published results with on-going model development.

Limitations

The model which has been presented has been limited to some mechanical factors which may affect the maternal blood flow. It is possible that other factors play some part in the control of this flow. For example, epinephrine released by the mother and/or the fetus in response to the stress of labor might change the vascular resistances. The uterine volume change which has been linked to the maternal placental blood flow may interact with the previously mentioned uterine wall thickening and muscle layer shifting.

The sluice flow formulation rests on the superficial similarity between the placenta/uterus arrangement and the laboratory experiments described by Holt (8).

The validity of the model rests entirely on the placental volume increase produced and on the cessation of arterial and venous blood flow found near the midpoint of a contraction.

Extension of the model for research and utilitarian purposes will be hampered by several factors. At present there is little available data against which to test the behavior of the model. Therefore modifications and alternatives cannot be chosen with any degree of confidence. Research with animal subjects is expensive and difficult and the applicability of the animal research to the human situation is always open to question.

The lack of non-invasive measurement methods suitable for use on humans severely limits research in this area. Since labor and delivery is not considered a pathological high risk state, the risk added by a research project must be considered negligible before it can be initiated. It would seem that labor and delivery research would greatly benefit from a multi-disciplinary approach because of the complexity of the mechanisms involved and the difficulties placed in the way of experimentation.

Prime Contribution

The most important contribution this thesis makes to the body of knowledge concerning the effect of labor on blood flow to the fetus is the explicit statement of a relation between the forces responsible for the delivery and the interruption of blood flow which accompanies those forces.

Regardless of the actual form of the flow equations, the basic behavior of the model is determined by the relationship between the intrauterine pressure and the pressure which controls the blood flow. The concept of the non-isometric contraction links these two pressures and future research should be directed at increasing our understanding of this linkage. Explicit, quantitative relationships between intrauterine pressure and placental blood flow would help the transition of fetal monitoring from an art to a science, to the benefit of mother, fetus and clinician.

REFERENCES

1. Abrams, R., Curet, L.B., Mann, L., Barron, D.H.: Uterine weight and intrauterine pressure in nonpregnant sheep, Am. J. Physiol. 215:1143-1145, 1968.

2. Assali, N.S., Brinkman, C.R.: The uterine circulation and its control. In Respiratory Gas Exchange and Blood Flow in the Placenta, ed. L.D. Longo and H. Bartels, pg. 121, U.S. Government Printing Office, 1972.

3. Assali, N.S., Holm, L., Parker, H.: Regional blood flow and vascular resistance in response to oxytocin in the pregnant sheep and dog, J. Appl. Physiol. 16:1087-1092, 1961.

4. Butler, L., Longo, L., Power, G.: Placental blood flows and oxygen transfer during uterine contractions: a mathematical model, J. Theor. Biol. 61:81-95, 1976.

5. Greiss, F.C.: Effect of labor on uterine blood flow, Am. J. Obstet. Gynecol. 93:917-923, 1965.

6. Hellman, L.M., Pritchard, J.A.: Williams Obstetrics, 14th edition, pg. 240, Appleton Century Crofts, New York, 1971.

7. Hellman, L.M., Pritchard, J.A.: Williams Obstetrics, 14th edition, pg. 355, Appleton Century Crofts, New York, 1971.

8. Holt, J.: Flow through collapsible tubes and through in situ veins, IEEE Trans. Bio-Med. Eng. BME-16, 274-283, 1969.

9. Huddleston, J.F., Perlis, H.W., Macy, J., Myers, R.E., Flowers, C.E.: The prediction of fetal oxygenation by an on-line computer analysis of fetal monitor output, Am. J. Obstet, Gynecol. 128: 599-605, 1977.

10. Lopez-Muniz, R., Stephens, N.L., Bromberger-Barnea, B., Permutt, S., Riley, R.L.: Critical closure of pulmonary vessels analyzed in terms of Starling resistor model, J. Appl. Physiol. 24:625-635, 1968.

11. Moll, W.: Gas exchange in concurrent, countercurrent flow systems. The concept of the fetoplacental unit. In Respiratory Gas Exchange and Blood Flow in the Placenta, ed. L.D. Longo and H. Bartels, pg. 281, U.S. Government Printing Office, 1972.

12. Myers, R.E., Mueller-Heubach, E., Adamsons, K.: Predictability of the state of fetal oxygenation from a quantitative analysis of the components of late deceleration, Am. J. Obstet. Gynecol. 115:1083-1094, 1973.

13. Novy, M.J.: The effect of sustained uterine contractions on myometrial and placental blood flow in the rhesus monkey. In Respiratory Gas Exchange and Blood Flow in the Placenta, ed. L.D. Longo and H. Bartels, pg. 143, U.S. Government Printing Office, 1972.

14. Perlis, H.W., Bearden, C.V., Germann, M.H.: Automated prediction of fetal distress, Proc. San Diego Biomed. Symp. 14:339-341, 1975.

15. Power, G.G.: The Placental Sluice: Maternal effects on the fetal circulation. In Respiratory Gas Exchange and Blood Flow in the Placenta, ed. L.D. Longo and H. Bartels, pg. 191, U.S. Government Printing Office, 1972.

16. Ramsey, E.M., Martin, C.B., McGaughey, H.S., Kaiser, I.H., Donner, M.W.: Venous drainage of the placenta in rhesus monkeys: radiographic studies, Am. J. Obstet. Gynecol. 95: 948-955, 1966.

17. Scheffs, J., Vasicka, A., Li, C., Solomon, N., Siler, W.: Uterine blood flow during labor, Obstet. Gynecol. 38:15-24, 1971.

APPENDIX

CSMP Program

The following page is an actual listing of the CSMP program as it existed after the last simulation run.

```
00010 PARAMETER ARTP=100.0, VENP=10.0
00020 PARAMETER ARTR=3.0,VENR=3.0
00030 PARAMETER VMAX=100.0,GAMMA=2.0,DELTA=3.0
00040 PARAMETER PEAK=80.0,SLOPE=300.0
00050 PARAMETER KAY=0.8
00060 PARAMETER PLACR=3.0
00070 PARAMETER VOL=90.0
00080 *CONTRACTION GENERATOR STARTS HERE
00090 DYNAMIC
00100 A=IMPULS(5.0,5.0)
00110 B=PULSE(0.5,A)
00120 C=IMPULS(5.5,5.0)
00130 D=PULSE(0.5,C)*(-1.0)
00140 E=B+D
00150 F=INTGRL(0.0,E)
00160 SQUEEZ=LIMIT(0.0,PEAK,F*SLOPE)
00170 SQ1=(SQUEEZ**(4.0/3.0))*KAY
00180 *INPUT VALVE SEQUENCE STARTS HERE
00190 PROCEDURE FLIN=BLOCKA(ARTP,PLACP,SQ1,ARTR,PLACR)
00200 IF((ARTP .GT. PLACP).AND.(PLACP .GT. SQ1)) GO TO 10
00210 IF((ARTP .GT. SQ1).AND.(SQ1 .GT. PLACP)) GO TO 20
00220 IF((SQ1 .GT. ARTP).AND.(ARTP .GT. PLACP)) GO TO 30
00230 IF((SQ1 .GT. PLACP).AND.(PLACP .GT. ARTP)) GO TO 30
00240 IF((PLACP .GT. ARTP).AND.(ARTP .GT. SQ1)) GO TO 10
00250 IF((PLACP .GT. SQ1).AND.(SQ1 .GT. ARTP)) GO TO 40
00260 10 FLIN=(ARTP-PLACP)/(ARTR+PLACR)
00270 GO TO 50
00280 20 FLIN=(ARTP-SQ1)/(ARTR+PLACR)
00290 GO TO 50
00300 30 FLIN=0.0
00310 40 FLIN=(SQ1-PLACP)/(PLACR+ARTR)
00320 50 CONTINUE
00330 ENDPRO
00340 *OUTPUT VALVE SEQUENCE STARTS HERE
00350 PROCEDURE FLOUT=BLOCKB(PLACP,VENP,SQ1,PLACR,VENR)
00360 IF((PLACP .GT. VENP).AND.(VENP .GT. SQ1)) GO TO 11
00370 IF((PLACP .GT. SQ1).AND.(SQ1 .GT. VENP)) GO TO 21
00380 IF((SQ1 .GT. PLACP).AND.(PLACP .GT. VENP)) GO TO 31
00390 IF((VENP .GT. PLACP).AND.(PLACP .GT. SQ1)) GO TO 11
00400 IF((VENP .GT. SQ1).AND.(SQ1 .GT. PLACP)) GO TO 41
00410 IF((SQ1 .GT. VENP).AND.(VENP .GT. PLACP)) GO TO 31
00420 11 FLOUT=(PLACP-VENP)/(PLACR+VENR)
00430 GO TO 51
00440 21 FLOUT=(PLACP-SQ1)/(PLACR+VENR)
00450 GO TO 51
00460 31 FLOUT=0.0
00470 GO TO 51
00480 41 FLOUT=(SQ1-VENP)/(VENR+PLACR)
00490 51 CONTINUE
00500 ENDPRO
00510 * VOLUME SEQUENCE STARTS HERE
00520 COMPLI=((PLAVOL/GAMMA)*ALOG(VMAX/PLAVOL))**(1.0/DELTA)
00530 PLACP=(PLAVOL/COMPLI)+SQUEEZ
00540 PLAVOL=INTGRL(VOL,(FLIN-FLOUT))
00550 TIMER FINTIM=10.0, OUTDEL=0.1
00560 PRTPLT PLAVOL,FLIN,FLOUT,PLACP,SQUEEZ
00570 END
00580 STOP
00590 ENDJOB
END OF DATA
```

CSMP PROGRAM NOTES

See Table 1 for correspondence between equation variables and CSMP variables.

Line 10 to Line 70	Sets up initial conditions and variable values.
Line 100 to Line 170	Creates the square wave by combining two opposite going pulses, integrates the square wave and limits its peak to form the intrauterine pressure curve and the effective sluice pressure curve as detailed in EQ. 17 and 18.
Line 200 to Line 310	Selects the input flow relationship according to the conditions detailed in EQ. 6, 7, 8 and 9.
Line 360 to Line 480	Selects the output flow relationship according to the conditions detailed in EQ. 13, 14, 15 and 16.
Line 520 to Line 540	Calculates the placental compliance, placental pressure and placental volume as shown in EQ. 10, 11 and 12.
Line 550	Determines the length of each simulation, the integration interval and the output plot interval.
Line 560	Selects the variables to be plotted on the high speed printer.

See IBM publication GH20-0367-3, revised 1971.

GRADUATE SCHOOL
UNIVERSITY OF ALABAMA IN BIRMINGHAM
DISSERTATION APPROVAL FORM

Name of Candidate Howard William Perlis

Major Subject Biophysical Sciences

Title of Dissertation A Mathematical Model of Placental Blood Flow

Dissertation Committee:

Chairman

Director of Graduate Program

Dean, UAB Graduate School

Date 24 March 1978